

Structural and electronic properties of boron nitride thin films containing silicon

Cite as: Journal of Applied Physics **84**, 5046 (1998); <https://doi.org/10.1063/1.368752>
Submitted: 25 June 1998 • Accepted: 28 July 1998 • Published Online: 14 October 1998

C. Ronning, A. D. Banks, B. L. McCarson, et al.



View Online



Export Citation

ARTICLES YOU MAY BE INTERESTED IN

[Electric conductivity of boron nitride thin films enhanced by in situ doping of zinc](#)
Applied Physics Letters **89**, 112124 (2006); <https://doi.org/10.1063/1.2354009>

[Electrical transport properties of Si-doped hexagonal boron nitride epilayers](#)
AIP Advances **3**, 122116 (2013); <https://doi.org/10.1063/1.4860949>

[Epitaxially grown semiconducting hexagonal boron nitride as a deep ultraviolet photonic material](#)
Applied Physics Letters **98**, 211110 (2011); <https://doi.org/10.1063/1.3593958>



Applied Physics
Reviews

Read. Cite. Publish. Repeat.

19.162
2020 IMPACT FACTOR*

Structural and electronic properties of boron nitride thin films containing silicon

C. Ronning,^{a)} A. D. Banks, B. L. McC Carson, R. Schlessner, Z. Sitar,
and R. F. Davis

*Department of Materials Science and Engineering, North Carolina State University, Raleigh,
North Carolina 27965*

B. L. Ward and R. J. Nemanich

Department of Physics, North Carolina State University, Raleigh, North Carolina 27965

(Received 25 June 1998; accepted for publication 28 July 1998)

The incorporation of silicon into boron nitride films (BN:Si) has been achieved during ion beam assisted deposition growth. A gradual change from cubic boron nitride (*c*-BN) to hexagonal boron nitride (*h*-BN) was observed with increasing silicon concentration. Ultraviolet photoelectron spectroscopy, field emission, and field emission electron energy distribution experiments indicated that the observed electron transport and emission were due to hopping conduction between localized states in a band at the Fermi level for the undoped *c*-BN films and at the band tails of the valence band maximum for the BN:Si films. A negative electron affinity was observed for undoped *c*-BN films; this phenomenon disappeared upon silicon doping due to the transformation to *h*-BN. No shift of the Fermi level was observed in any BN:Si film; thus, *n*-type doping can be excluded.

© 1998 American Institute of Physics. [S0021-8979(98)03421-5]

I. INTRODUCTION

Thin films of cubic boron nitride (*c*-BN) have been investigated extensively for their potential in tribological applications, as this phase possesses a hardness second only to diamond, is stable to 1100 °C, and is chemically inert to oxygen and ferrous materials. It is also a candidate semiconductor material, as small crystals have been successfully doped during high-pressure/high-temperature (HPHT) synthesis both *p*- and *n*-type with Be and Si, respectively, with a concomitant reduction in the resistivity.¹ Intrinsic *c*-BN has been reported to exhibit a negative electron affinity (NEA).² The smooth surface of *c*-BN films provides a potential advantage for the fabrication of electronic devices and flat field emitters relative to that of the rough polycrystalline chemical vapor deposition diamond films.

Undoped *c*-BN films exhibit a resistivity from 10^9 – 10^{11} Ω cm.^{3–5} Contradictory claims have been made concerning the conduction mechanism. *n*-type⁶ and *p*-type⁷ conduction as well as Frenkel–Poole emission^{4,5} have been reported for undoped *c*-BN films. Attempts to achieve *n*-type doping in BN films have included the incorporation of S, C, and Si. The addition of S resulted in eight orders of magnitude lower resistivity and *n*-type conductivity; however, the field emission properties of this material were only slightly enhanced.³ Insufficient results have been published regarding the efficacy of C as a *n*-type dopant.⁸ The incorporation of Si has been extensively studied by Zhao *et al.*⁹ to improve the mechanical properties. Structural changes were observed; however, the electronic properties and the potential of these films as field emitters were not considered.

The synthesis of pure phase and monocrystalline *c*-BN films has been achieved only via high-temperature, high-pressure methods.¹ Films containing varying amounts of *c*-BN have been synthesized using numerous techniques (for a review see Ref. 10). The microstructure of each film usually displays a three phase progression from the substrate to (i) an amorphous layer which contains a mixture of substrate, boron, and nitrogen atoms, (ii) a textured hexagonal boron nitride (*h*-BN) layer, and (iii) a textured polycrystalline (crystallite size: 5–50 nm) *c*-BN layer.¹¹ The nucleation of the cubic phase has been achieved only by ion bombardment, and sharp thresholds in ion energy and growth temperature separate the growth parameters of *h*-BN and *c*-BN.¹² The growth mechanism of BN is not well understood, and there have been several models proposed for the nucleation of *c*-BN.¹³

The results obtained in this research from *c*-BN thin films containing intentionally added silicon are described in the following sections. Ion beam assisted deposition (IBAD), a common technique with proven success in *c*-BN synthesis,¹⁴ was employed in this study. The potential for field emission of *h*-BN, a related wide band gap material, was also investigated.

II. EXPERIMENT

The deposition of BN was achieved via simultaneous evaporation of boron using an electron beam evaporator and the bombardment of the depositing metal with both nitrogen and argon ions generated in a Kaufman-type ion gun. A schematic of the deposition system is shown in Fig. 1. The parameters used for the preparation of the undoped *h*-BN and *c*-BN films were similar to those used by Kester and Messier¹⁴ and Reinke *et al.*,¹⁵ and the same boundaries for

^{a)}Electronic mail: Carsten.Ronning@uni-konstanz.de

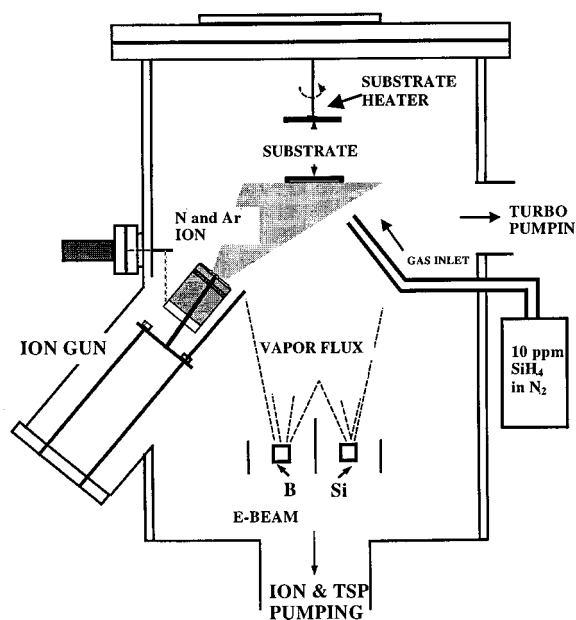


FIG. 1. Schematic of the IBADEP-deposition system. Boron and silicon were evaporated by two separate *e*-beam evaporators. Simultaneously the substrate was bombarded with nitrogen and argon ions. Doping of BN films could be also achieved by a flow of a mixture of 10 ppm silane (SiH_4) in nitrogen to the surface during film deposition.

h-BN and *c*-BN nucleation and growth were established. An ion energy of 600 eV, an ion/boron arrival ratio of two and a substrate temperature of 500 °C were used to prepare all films described in this study. These conditions yielded undoped BN films containing 70%–90% of the cubic phase. Typical film thicknesses were 100–200 nm.

The substrates were cleaned with acetone before transfer into the IBADEP system and sputter cleaned *in situ* with 1 keV Ar^+ ions immediately prior to film deposition. This procedure resulted in a significant improvement in the adhesion of the *c*-BN films. Even films with a very high concentration of the cubic phase content have not delaminated after four months.

Silicon was introduced into the films at 500 °C via a mixture of 10 ppm silane (SiH_4) in nitrogen (Fig. 1), and a mass flow controller determined the flow rate. The flow rate of the SiH_4 gas mixture was varied from 0–7 sccm, and the *c*-BN growth parameters were maintained constant. Above 7 sccm the pressure in the chamber exceeded 5×10^{-4} Torr, which caused the ion source discharge to become unstable. The simultaneous electron beam evaporation of Si was investigated as an alternate method of introduction of this element.

Secondary ion mass spectroscopy (SIMS), infrared spectroscopy (FTIR), x-ray and ultraviolet photoelectron spectroscopy (XPS and UPS, respectively), field emission (FE), and field emission energy distribution (FEED) experiments were performed to analyze the film composition and the structural and electronic changes of the BN films induced by the added silicon.

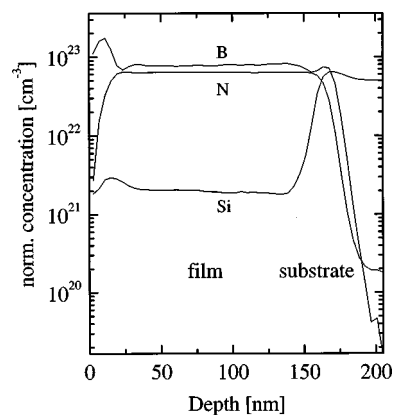


FIG. 2. SIMS depth profiles of the boron, nitrogen, and silicon signals of a sample grown under a flow rate of 7 sccm and *c*-BN conditions.

III. RESULTS AND DISCUSSION

A. Composition and microstructure

The composition of the films prepared with the flow of SiH_4 was checked using SIMS. Figure 2 shows the boron, nitrogen, and silicon depth profiles of a sample, which was grown under a total flow rate of 7 sccm. Approximately $2 \times 10^{21} \text{ cm}^{-3}$ (4 at. %) silicon atoms were uniformly incorporated throughout the film thickness. A silicon concentration of $3 \times 10^{20} \text{ cm}^{-3}$ (0.6 at. %) was determined for a BN film grown under 2 sccm gas flow, while undoped films had less than 10^{19} cm^{-3} (<0.02 at. %) incorporated silicon atoms. This clearly demonstrates that BN films with uniform and low concentrations in the percentage range of silicon can be easily prepared under these experimental conditions.

Simultaneous co-evaporation of silicon during BN film growth was used to prepare films containing higher concentrations of silicon. These films were examined *in vacuo* by XPS. Boron, nitrogen, silicon, and argon (<2%) signals have been observed; however, no carbon or oxygen contamination was present. Approximate stoichiometries to $\text{B}_{0.7}\text{Si}_{0.3}\text{N}$ were realized.

Figure 3 shows the B 1s core level spectra as a function of silicon concentration for BN:Si films prepared by co-evaporation. The peak at ≈ 190.5 eV agrees well with reported binding energy for boron in BN.^{16,17} The intensity of the line at ≈ 188 eV was negligible for undoped BN films, but increased for higher silicon concentrations (see Fig. 3). This component can be attributed to boron atoms bonded to at least one silicon atom. The binding energy is in good agreement with reported binding energies of borides.¹⁸ The same behavior was observed for BN:Si films prepared under the gas flow of SiH_4 . The binding energy of the Si 2p core level was ≈ 101.6 eV, which is more typical for nitrides than for silicides;¹⁸ however, the line was very broad having a full width at half maximum of ≈ 3 eV. Silicon should substitute for boron in *c*-BN as a dopant; however, these results show that Si is also bonded to boron by replacing nitrogen, which may reduce its electronic doping efficiency.

A gradual decrease in *c*-BN content was observed with increasing silicon concentration for films prepared under the flow of the silane mixture, as shown in Fig. 4. The absorp-

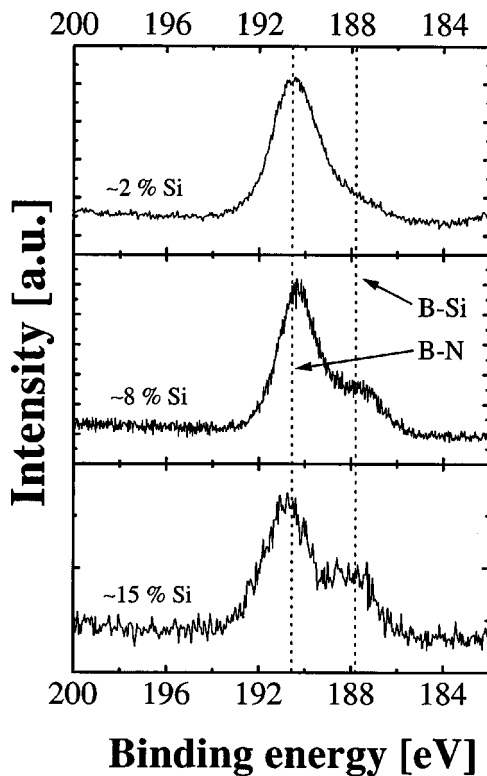


FIG. 3. B $1s$ core level spectra of BN films prepared by co-evaporation of silicon as a function of silicon concentration.

tion line at 1090 cm^{-1} associated with the transverse optical mode of *c*-BN decreased with increasing flow rates; while the *h*-BN absorption lines at 780 and 1390 cm^{-1} increased. We observed the same behavior for BN:Si films prepared by co-evaporation of silicon. These results demonstrate that the *c*-BN structure is replaced by a *h*-BN phase with increasing silicon concentration, which is in agreement with the results of Zhao and co-workers.⁹

B. Electron transport and emission

Ex situ UPS measurements of an undoped *c*-BN and BN:Si sample (SiH_4N_2 flow rate = 2 sccm, i.e., in the intermediate range shown in Fig. 4) were taken in a different ultrahigh vacuum (UHV) system and are shown in Fig. 5. An *in vacuo* radio frequency (rf) H plasma treatment was used prior to the measurements to clean the surface. During this step the surface was also H-terminated. The UPS spectra were measured while the sample was biased by 2 V to reveal the full width of the electron energy spectrum and to eliminate artifacts of the electron analyzer. The NEA of the undoped *c*-BN sample is clearly visible at a binding energy of $\approx 15.7\text{ eV}$, which is in agreement with Ref. 2. Undoped *c*-BN samples, which were not cleaned with the H plasma, did not exhibit a NEA, but a low positive electron affinity. The valence band maximum (VBM) was located $\approx 1\text{ eV}$ below the Fermi level, as shown in the insert of Fig. 5. This results in a band gap of $\approx 5.5\text{ eV}$ for the undoped *c*-BN films. This is lower than the band gap of 6.2 eV of HPHT crystals.¹ No NEA was observed for the BN:Si films; however, the high intensity at a binding energy around 14 eV

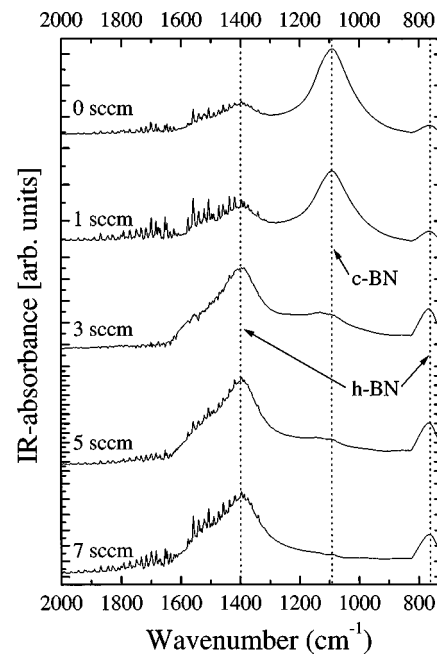


FIG. 4. FTIR-absorbance spectra of BN films prepared under varying SiH_4 flows.

shows that the positive electron affinity is low. Extrapolating the intensity to zero on the left-hand side of the spectrum yielded a width of $\approx 15.85\text{ eV}$, which results in an even smaller band gap of $\approx 5.35\text{ eV}$. The position of the VBM was also determined $\approx 1\text{ eV}$ below the Fermi level. Therefore, no shift of the Fermi level within the band gap occurred upon Si incorporation.

Current–voltage (I – V) FE curves were obtained *in vacuo* after the UPS measurements. Figure 6 shows the measured I – V curves of the same BN:Si sample for different

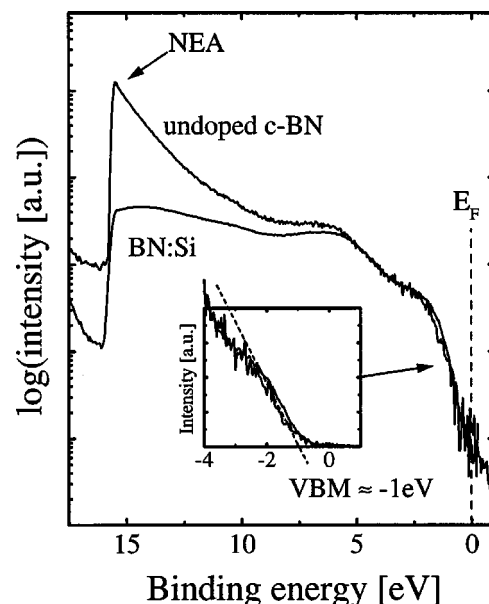


FIG. 5. UPS HeI spectra of an undoped *c*-BN sample and a BN:Si sample grown under a flow rate of 2 sccm. An *in vacuo* rf H plasma treatment was used prior to the measurements to clean the surface. The UPS spectra were measured while the sample was biased by 2 V.

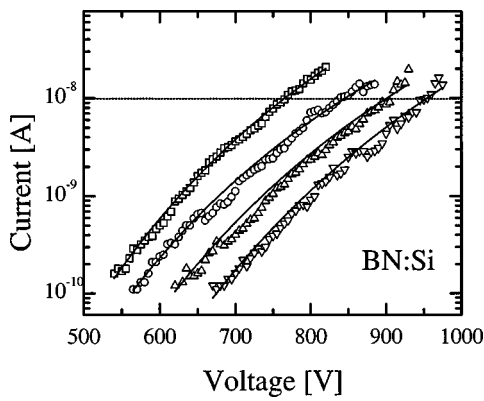


FIG. 6. I - V field emission curves taken under UHV conditions of the same BN:Si sample measured by UPS and grown under a flow of 2 sccm for different sample-anode distances. The solid lines represent fits of the Fowler-Nordheim equation to the measured data.

distances between the flat sample and a molybdenum anode. The rod-shape anode (curvature=5.5 mm) had a diameter of 3 mm. The data points followed well the Fowler-Nordheim dependence,¹⁹ which was fitted to the measured data and plotted as a solid line in Fig. 6. Figure 7 shows the threshold voltage for a current of 10 nA extracted from Fig. 6 as a function of the relative distance between different measurements. A linear fit of this plot determines the threshold field for the electron emission. Improved accuracy for the determination of the threshold field is achieved by this procedure, since it is always a problem to measure the exact distance between the sample and the anode. The fit in Fig. 7 indicates a threshold field for the BN:Si sample of ≈ 133 V/ μ m. This value is slightly below that measured for uncoated Si; however, for undoped c -BN a lower threshold field of 102 V/ μ m was determined, as shown in Fig. 7. No damage to the flat films occurred during these measurements; however, we observed a high degree of damage after further measurements at smaller distances. This “crater”-shaped damage was induced by an arc discharge between the sample and the anode during the FE measurements. This event was easily perceived by a strong increase of the emission current and a

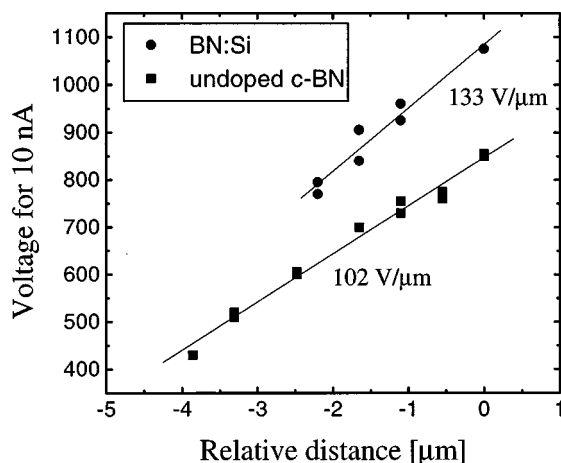


FIG. 7. Threshold voltages for a field emission current of 10 nA extracted from Fig. 5 as a function of relative distance. A linear fit determines the threshold field.

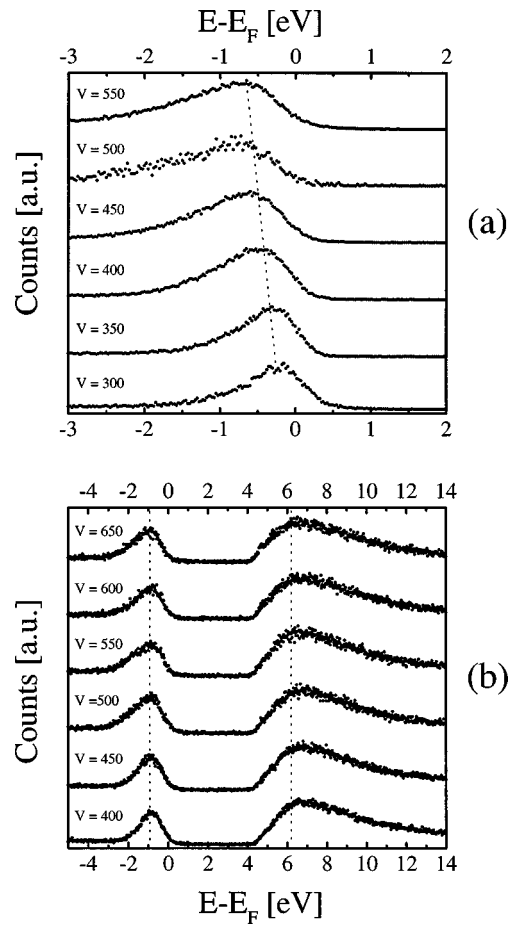


FIG. 8. (a) FEED spectra of a c -BN film deposited on Si. Data were recorded at several different applied voltages. (b) Simultaneous FEED and photoelectron emission spectra from a c -BN:Si grown at a flow rate of 2 sccm of the silane mixture.

strong decrease of the threshold field, which is caused by a much higher field enhancement factor of the damaged region as the arc ablates material from the initially smooth surface.

FEED measurements were performed to determine the mechanism and origin of the field emitted electrons in the undoped and Si-containing c -BN films. This technique has been described in detail elsewhere.²⁰ Figure 8(a) shows that the kinetic energy of the emitted electrons measured relative to the Fermi level ($E - E_F$) from the undoped c -BN decreased linearly with the applied voltage. Extrapolation of the FEED peak position to a flatband condition (no applied field) leads to an intercept at ≈ 0 eV. This demonstrates that the field-emitted electrons originated from the Fermi level of the undoped film. Simultaneous field and photoelectron emission (x rays, $h\nu = 1.4$ keV, sample biased) measurements obtained from a c -BN:Si film, prepared using a flow rate of 2 sccm are shown in Fig. 8(b). No shift of the kinetic energy ($E - E_F$) of the emitted electrons was observed as function of applied voltage; this is due to the larger conductivity of the film. The intercept is around -1 eV, which indicates that the emission of the electrons occurred ≈ 1 eV below the Fermi level. Considering the UPS data noted above, the emitted electrons originated from the valence band maximum for BN:Si films. The results of photoelectron

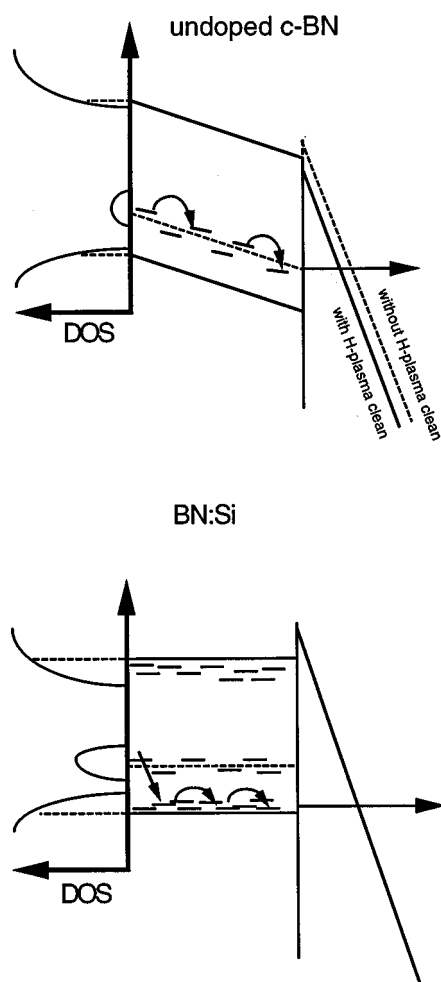


FIG. 9. Possible mechanism for the electron transport and emission from (top) undoped *c*-BN and (bottom) BN:Si thin films. A corresponding density of states for each scenario is drawn on the left-hand side.

measurements with $h\nu = 1.4$ keV on the biased sample are shown in Fig. 8(b) and reveal a vacuum level of about 6.2 eV above the Fermi level of the film. This results in a small positive electron affinity of ≈ 1.5 eV, which is in good agreement with the UPS measurements (Fig. 5). A variety of *c*-BN and *h*-BN films with different silicon concentrations as well as *c*-BN and *h*-BN samples prepared by the co-evaporation of silicon and boron were also measured. In all cases, similar results were obtained, and the measurements displayed in Fig. 8 are representative of these results.

We propose the scenario illustrated in Fig. 9 to explain the electron field emission from BN thin films. It is most probable that electron transport through the undoped *c*-BN films is due to hopping conduction at localized states in a band at the Fermi level, and the emission of the electrons occurred at this position in the band gap. In this case, a NEA only slightly enhanced the electron emission compared to a low positive electron affinity. This suggestion is supported by the fact that the width of the FEED peaks of the field emitted electrons increased with increasing voltage [Fig. 8(a)] and by the work reported in Ref. 4. The localized states in the *c*-BN material are due to the high density of grain

boundaries and defects within the nanosized (10–30 nm) crystals of the film.¹²

We have shown that the incorporation of silicon in IBAD prepared BN material does not shift the Fermi level; however, we suggest the creation of additional localized states in the band gap and band tails at the valence band maximum as well as at the conduction band minimum, as shown in Fig. 9. The probability for thermalization of the electrons during transport through the film into these additional states at the band tail of the valence band increases relative to the undoped *c*-BN films. Therefore, electron transport and emission occurred in the BN:Si films through the band tails of the valence band maximum. This also explains the higher, measured threshold field in the *I*–*V* field emission experiments after silicon incorporation. A microstructural reason for the creation of these new states may be that *c*-BN is gradually replaced by *h*-BN upon silicon incorporation. Another reason that *n*-type doping did not occur for the BN:Si films is that a significant amount of the incorporated silicon is also bonded to boron and did not replace boron, as has been shown in Sec. III A.

IV. CONCLUSIONS

Thin films of BN:Si were grown using IBAD. The successful incorporation of silicon during film growth was achieved using two different techniques. Silicon concentrations to 4 at. % were obtained by flowing a mixture of 10 ppm SiH₄ in nitrogen over the surface of the growing film; whereas, concentrations to 15 at. % were realized via co-evaporation of silicon. A gradual change from *c*-BN to *h*-BN was observed with increasing silicon concentration. Silicon should substitute boron in *c*-BN as a dopant; however, Si was also bonded to boron by replacing nitrogen, which also effectively prevented *n*-type doping. It is most probable that electron transport and emission were due to hopping conduction at localized states in a band at the Fermi level in the undoped *c*-BN films and at the band tails of the valence band maximum in the BN:Si films. This explains the observed poorer field emission properties of the BN:Si films relative to undoped *c*-BN films. None of the BN:Si films showed a significant shift of the Fermi level toward the conduction band minimum in the UPS and FEED measurements; thus, *n*-type doping can be excluded.

ACKNOWLEDGMENTS

This work was supported by the ONR under Contract No. N00014-92-J-1477 (M. Yoder, technical monitor). One of the authors (C.R.) is grateful for funding by the DFG (Ro 1198/2-1). Another author (R.D.) was supported in part by the Kobe Steel, Ltd. Professorship.

¹O. Mishima, J. Tanaka, S. Yamaoka, and O. Fukunaga, *Science* **238**, 181 (1987); *Appl. Phys. Lett.* **53**, 962 (1988).

²M. J. Powers, M. C. Benjamin, L. M. Porter, R. J. Nemanich, R. F. Davis, J. J. Cuomo, G. L. Doll, and S. J. Harris, *Appl. Phys. Lett.* **67**, 3912 (1995).

³T. Sugino, S. Kawasaki, K. Tanioka, and J. Shirafuji, *Appl. Phys. Lett.* **71**, 2704 (1997); *Diamond Relat. Mater.* **7**, 632 (1998).

- ⁴C. Ronning, E. Dreher, H. Feldermann, M. Gross, M. Sebastian, and H. Hofsäss, *Diamond Relat. Mater.* **6**, 1129 (1997).
- ⁵J. Szmids, A. Jakubowski, A. Michalski, and A. Rusek, *Thin Solid Films* **110**, 7 (1983); *Diamond Relat. Mater.* **1**, 681 (1992).
- ⁶A. R. Phani, S. Manorama, and V. J. Rao, *Semicond. Sci. Technol.* **10**, 1520 (1995).
- ⁷D. Litvinov, C. A. Taylor II, and R. Clarke, *Diamond Relat. Mater.* **7**, 360 (1998).
- ⁸R. W. Pryor and H. Busta, *J. Appl. Phys.* **82**, 5148 (1997); *Appl. Phys. Lett.* **68**, 1802 (1996); *Mater. Res. Soc. Symp. Proc.* **416**, 425 (1996).
- ⁹X.-A. Zhao, C. W. Ong, K. F. Chan, Y. M. Ng, Y. C. Tsang, C. L. Choy, and P. W. Chan, *J. Vac. Sci. Technol. A* **15**, 2297 (1997).
- ¹⁰P. B. Mirkarimi, K. F. McCarty, and D. L. Medlin, *Mater. Sci. Eng., R.* **21**, 1 (1997).
- ¹¹R. F. Davis, D. J. Kester, and K. S. Ailey, in *Chemical Vapor Deposition of Refractory Metals and Ceramics III*, edited by B. M. Gallois *et al.* [*Mater. Res. Soc. Symp. Proc.* **363**, 139 (1995)]; *J. Mater. Res.* **8**, 1213 (1993).
- ¹²H. Hofsäss, H. Feldermann, M. Sebastian, and C. Ronning, *Phys. Rev. B* **55**, 13230 (1997).
- ¹³H. Hofsäss, H. Feldermann, R. Merk, M. Sebastian, and C. Ronning, *Appl. Phys. A: Mater. Sci. Process.* **66**, 153 (1998), and references therein.
- ¹⁴D. J. Kester and R. Messier, *J. Appl. Phys.* **72**, 504 (1992).
- ¹⁵S. Reinke, M. Kuhr, W. Kulish, and R. Kassing, *Diamond Relat. Mater.* **4**, 272 (1995).
- ¹⁶K. S. Park, D. Y. Lee, K. J. Kim, and D. W. Moon, *Appl. Phys. Lett.* **70**, 315 (1997).
- ¹⁷R. Trehan, Y. Lifshitz, and J. W. Rabalais, *J. Vac. Sci. Technol. A* **8**, 4026 (1990).
- ¹⁸*Handbook of X-ray Photoelectron Spectroscopy*, edited by J. Chastain (Perkin-Elmer, Eden Prairie, MN, 1992), p. 215.
- ¹⁹R. H. Fowler and L. W. Nordheim, *Proc. R. Soc. London, Ser. A* **119**, 173 (1928).
- ²⁰R. Schlessler, M. T. McClure, B. L. McCarson, and Z. Sitar, *J. Appl. Phys.* **82**, 5763 (1997).